

## An atomistic study on the stretching of nanowires

This article has been downloaded from IOPscience. Please scroll down to see the full text article.

1997 J. Phys.: Condens. Matter 9 10843

(<http://iopscience.iop.org/0953-8984/9/49/005>)

View [the table of contents for this issue](#), or go to the [journal homepage](#) for more

Download details:

IP Address: 171.66.16.209

The article was downloaded on 14/05/2010 at 11:45

Please note that [terms and conditions apply](#).

## An atomistic study on the stretching of nanowires

H Mehrez†, S Ciraci†, C Y Fong†§ and Ş Erkoç‡

† Department of Physics, Bilkent University, Bilkent 06533, Ankara, Turkey

‡ Department of Physics, Middle East Technical University, Ankara, Turkey

Received 2 June 1997, in final form 29 September 1997

**Abstract.** In this work we present an atomic-scale investigation of elastic and plastic deformation, and force variations in metal nanowires that are pulled from their ends. The atomic simulations are performed by using a molecular dynamics method with an empirical two-body potential; the effect of the initial size, shape, temperature and rate of stretching on the necking and fracture are investigated. We find that the necking occurs mainly due to the formation of a new layer with a smaller cross-section after every structural yield, and concurrently the tensile force falls abruptly. The relationship between the atomic structure and the conductance of the wire is analysed by constructing a realistic potential for the neck in terms of a linear combination of atomic pseudopotentials and by calculating the conductance using the transfer matrix method. Our results show that the variation of the conductance is strongly correlated with the sudden structural changes in the neck, and reflects the quantization of electronic states in the neck, but not the quantization of the conductance.

### 1. Introduction

When the diameter of a metal wire is of the order of a nanometre, its discrete nature dominates over the continuum description, and the quantum behaviour of electrons is easily resolved at room temperature. Hence any atomic rearrangement during the plastic deformation or the necking would lead to detectable variations in the electronic and mechanical properties. Such an atomic-size connective neck was first realized by pushing a sharp metal STM tip towards a metal surface [1] to form a quantum point contact [2]. Later, much better control over the size and dimensions of the wires was obtained by pulling the STM tip after making a nanoindentation [3]. Such wires have been pulled off as long as 100–400 Å, and the narrowest parts have been reduced down to few atoms [4]. The variation of the ballistic conductance  $G$  [3–6] and yield strength  $\sigma_y$  [7, 8] with the stretch  $s$  of the wire have revealed interesting features. In such quantum structures the level spacings of electronic states are in the region of  $\sim 1$  eV, which, of course, reflects the electronic transport properties [2, 9]. There has been much dispute recently as to whether the conductance of a nanowire is really quantized and leads to a sharp step structure [5, 6]. Earlier theoretical work [2, 10–12] that attributed the sudden jumps of the  $G(s)$  curve to discontinuous (and irregular) changes of the cross-section at the contact (or at the neck) has been confirmed by recent experiments [7, 8] providing simultaneous measurements of  $G(s)$  and the variation of the tensile force,  $F_z(s)$ . It has been shown that the jumps of  $G(s)$  occur whenever  $F_z(s)$  decreases suddenly. With these results, it has become clear that the variation of  $G(s)$  is closely correlated with atomic rearrangements, and hence a detailed

§ On sabbatical leave from: University of California, Davis, CA, USA.

knowledge of the atomic structure during stretching is necessary for a better understanding of various features of  $G(s)$ .

In this work, we investigate atomic rearrangements in the course of stretching and explore their effects on the conductance of the nanowire. The stretching of the wire is simulated by using a classical molecular dynamics method to reveal atomic rearrangements and to calculate the  $F_z(s)$  curve. We examine the effect of the initial size, shape and temperature on the necking and fracture, and present a detailed analysis of the atomic structure that reveals interesting features. We calculate also the  $G(s)$  curve corresponding to the structure obtained from the molecular dynamics simulations, and compare it with the  $F_z(s)$  curve.

## 2. The method for the atomistic simulations

For a many-body system such as a nanowire, the classical molecular dynamics (MD) method using an empirical potential appears to be a feasible approach to performing large-scale atomistic simulations. These simulations have had reasonable success in revealing the response of materials to external force and in determining the atomic rearrangements induced therefrom [4, 11, 13]. In the present study, the interactions among the atoms of the wire are represented by an empirical potential function:

$$\Phi = D_1 \sum_{i < j} U_{ij}^{(1)} + D_2 \sum_{i < j} U_{ij}^{(2)} \quad (1)$$

which is formed from pair interactions only, and contains many-body contributions [14]. Two-body repulsive,  $U_{ij}^{(1)} = A_1 r_{ij}^{-\lambda_1} \exp(-\alpha_1 r_{ij}^2)$ , and attractive,  $U_{ij}^{(2)} = A_2 r_{ij}^{-\lambda_2} \exp(-\alpha_2 r_{ij}^2)$ , interaction functions are expressed in terms of the interatomic distances,  $r_{ij}$ . Here the exact pair-potential function  $U_{ij} = U_{ij}^{(1)} + U_{ij}^{(2)}$  and six parameters are determined by fitting it to the experimentally determined curve for the  $\text{Cu}_2$  dimer [14]. The parameters are:  $A_{1,2} = 110.766\,008, -46.164\,9783$ ;  $\lambda_{1,2} = 2.090\,459\,46, 1.498\,530\,83$ ; and  $\alpha_{1,2} = 0.394\,142\,248, 0.207\,225\,507$  (energy in eV, distance in Å). Then the values  $D_1 = 0.436\,092\,895$  and  $D_2 = 0.245\,082\,238$  are obtained by using the experimental cohesive energy and bulk stability condition [14]. The potential predicts the fcc structure as the most stable one among hcp (ideal), bcc, hcp (Zn), sc and diamond. The energy difference between the fcc and hcp (ideal) was small, but finite. This difference can be taken as a measure of the finite stacking fault energy. The bulk elastic constants,  $C_{11}$  and  $C_{12}$ , and bulk modulus,  $B$ , which are calculated by using this empirical potential, were found to be in good agreement with the experimental values. The results of the investigation of the cluster properties (such as the structural stability of clusters  $\text{Cu}_n$  with  $n = 3, 4, 5, 6, 7, 13-135$ , and their melting and dissociation for  $n = 13$  and  $n = 55$ ) were found to be in agreement with the available literature values (see reference [14] for further details and relevant references).

Here we deal with nanowires which are made initially from Cu(001) planes. The atomic planes lie in the  $(xy)$ -plane, and the  $z$ -axis is parallel to the [001] direction. Each of the nanowires has a neck that is connected to the shanks at both ends. The shanks have larger cross-sections relative to the neck. Each shank has six Cu(001) layers; the three end layers are rigid and are assumed to be connected to the external agent that applies the tensile stress (see the inset of figure 1). The atoms in the remaining three layers of the shank (that are adjacent to the end layers and connected to the neck from the other side) and those of the neck layers can be moved without constraint. The atoms in these movable layers are called dynamic atoms. In order to avoid the effects of the corners with low coordination numbers, the atomic layers are taken as quasi-circular. Here we deal with three types of

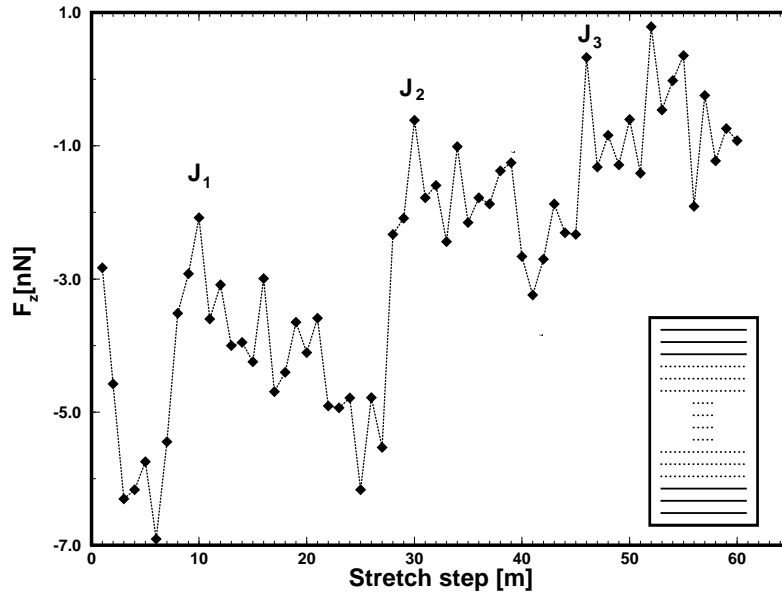


**Figure 1.** The tensile force versus the number of stretching steps  $m$  ( $s = m \Delta z$ ) calculated for the Cu(001) wire at  $T = 300$  K.  $J_1$ ,  $J_2$  and  $J_3$  indicate the abrupt reductions of the neck during the stretching. The inset gives a schematic representation of the initial, relaxed structure for the wide neck projected onto the  $(xz)$ -plane; continuous and dotted lines correspond to robust and dynamic layers, respectively.

nanowire, specified as wn (wide-neck), tn (thin-neck) and ttn wires (wires with tapered thin necks). Before stretching, the shank and neck layers of wn wires have  $\sim 145$  and 13 atoms, respectively, whereas the tn wire has a smaller cross-section and includes 41 and 5 atoms in the shank and neck layers, respectively. While the neck is connected to the shank discontinuously in wn and tn wires, the lower part of the shank of a ttn wire is tapered and makes a smooth connection to the neck. The stretch of the nanowire is realized by the sequential rigid translation of the end layers along the  $z$ -axis by increments of  $\Delta z$  either from both ends (for the ttn wire) or from one end while keeping the other end fixed (for the wn and tn wires); in this way a tensile force is generated. After  $m$  increments the nanowire is elongated by  $s = m \Delta z$ . Between two consecutive increments ( $m$  and  $m + 1$ ), the end layers become fixed, but the rest of the atoms in the wire (i.e. all of the dynamic atoms) are relaxed to attain their new equilibrium positions. In each relaxation step, the dynamic atoms are allowed to move under the interaction force generated from the empirical potential within a time interval of  $\Delta t = 0.9 \times 10^{-15}$  seconds and their new positions are determined by solving the equation of motion. The relaxation steps are repeated at least  $8 \times 10^3$  times between  $m$  and  $m + 1$  until the dynamic atoms reach a steady state. In order to keep the temperature at 300 K, the velocities of all of the dynamic atoms are rescaled at the end of every two steps of relaxation. Whether or not the dynamic atoms attained the steady-state condition is tested by further relaxing the structure over 2000 steps without rescaling the velocities after 8000 relaxation steps (where the velocities were scaled) and by examining the variation of the total potential energy and average temperature  $T$  thereafter. It is concluded that the relaxation and thermalization procedure is suitable, and hence the structure is properly equilibrated in the present study. The tensile force  $F_z$  (which is the attractive force between the fixed top three layers and the rest of the wire) is obtained

after averaging over the last 2000 steps, so the force fluctuations are minimized. A crucial issue to be aware of is that the velocity of the stretching used in the present simulations ( $\sim 1 \text{ m s}^{-1}$ ) is very much greater than the tip retraction rate ( $\sim 10^{-10} \text{ m s}^{-1}$ ) realized in STM experiments. In view of the agreement between experiment and the results obtained from the present simulations one can argue that the crucial parameters are  $\Delta z$  and  $\Delta t$ ; as long as they are kept small, the minimum-energy configuration attained by the system after 8000 relaxation steps can be close to that in the experiment.

### 3. Results

In this section we examine the atomic configuration and the force variations as functions of the stretch  $s$ . We start with the *wn* nanowire at  $T = 300 \text{ K}$ . The interlayer distance between the bulk Cu(001) layers is  $\sim 1.8 \text{ \AA}$ . The ideal layer structure of the wire (prior to any relaxation and stretching) exhibits the usual stacking sequence (A–B–A–B··) of the (001) atomic planes in the fcc lattice. Accordingly, the atoms of the B layers face the hollow sites, i.e. the centres of the square unit cells of the adjacent A layers (i.e. the centres of the primitive unit cells of the Cu(001) plane). This stacking, which is specified as the H-site registry, lowers the total energy. The variation of the tensile force with the stretch,  $s = m \Delta z$ , is calculated with  $\Delta z = 0.1 \text{ \AA}$  and is illustrated in figure 1. The  $F_z(m)$  curve displays small fluctuations and also abrupt jumps  $J_1, J_2, J_3$ . The tensile force normally increases with increasing  $m$  between two consecutive jumps  $J_m$  and  $J_{m+1}$ . This is the ‘quasi’-elastic stage. At the end of each elastic stage, the force decreases suddenly whenever the wire is stretched by approximately an interlayer distance. Once the stretch reaches the limits ( $m = 7, 27, 47$ ) of the elastic stages, the atomic structure of the neck becomes disordered and eventually a new layer with a smaller cross-section is generated (at  $m = 10, 28\text{--}30, 48$ ). In this way the strain energy and the tensile force are reduced, and the layer structure is recovered, but the neck becomes narrower. These are identified as the yielding stages. The present results exhibit the same trends as were obtained for different metal wires [4, 7, 8, 12, 15, 16].

Figure 2 shows side views of the atomic structure at various stages of the stretching. The first panel ( $m = 1$ ) illustrates the atomic structure of the wire that is relaxed at the beginning of the stretching. We take this as the starting point of the structure. Once the stretch reaches the value  $7 \Delta z$ , the layer structure suddenly disappears and the central region of the neck becomes disordered as is seen for  $m = 7$ . For  $m \geq 8$ , the layer structure is recovered via the formation of a new layer with a smaller cross-section (having eight atoms). The quasi-elastic stage starts after  $m = 10$  and continues until  $m = 26$ , whereupon the layer configuration persists but  $|F_z|$  increases with increasing  $m$ . The fluctuations of  $F_z$  are mainly due to local rearrangement of the atoms during stretching. The layer structure is destroyed again at  $m \sim 27$ , but it is recovered at  $m \sim 28$  with a new layer having a much smaller cross-section (three atoms). We note an interesting feature here: that the cross-section increases again with further stretching at  $m = 30$ ; an atom from the adjacent layer migrates to the narrowest layer, which then incorporates four atoms. As we show in the next section, this may cause an increase of  $G$  subsequent to a dip occurring at  $m = 28$ . Upon further increase of the stretching ( $m > 30$ ), after  $J_2$ , the third ‘quasi-elastic’ stage proceeds with stronger fluctuations due to there being fewer atoms at the neck. Here we note that the panel at  $m = 40$  has the *four* atoms of the neck rearranged to make two chains. Finally, one atom leaves the narrowest neck layer and is located in the wide spacing between the two central layers (panel  $m = 47$  in figure 2). At the end of these sequential processes the tensile force drops abruptly and eventually a connective neck of one single atom is formed

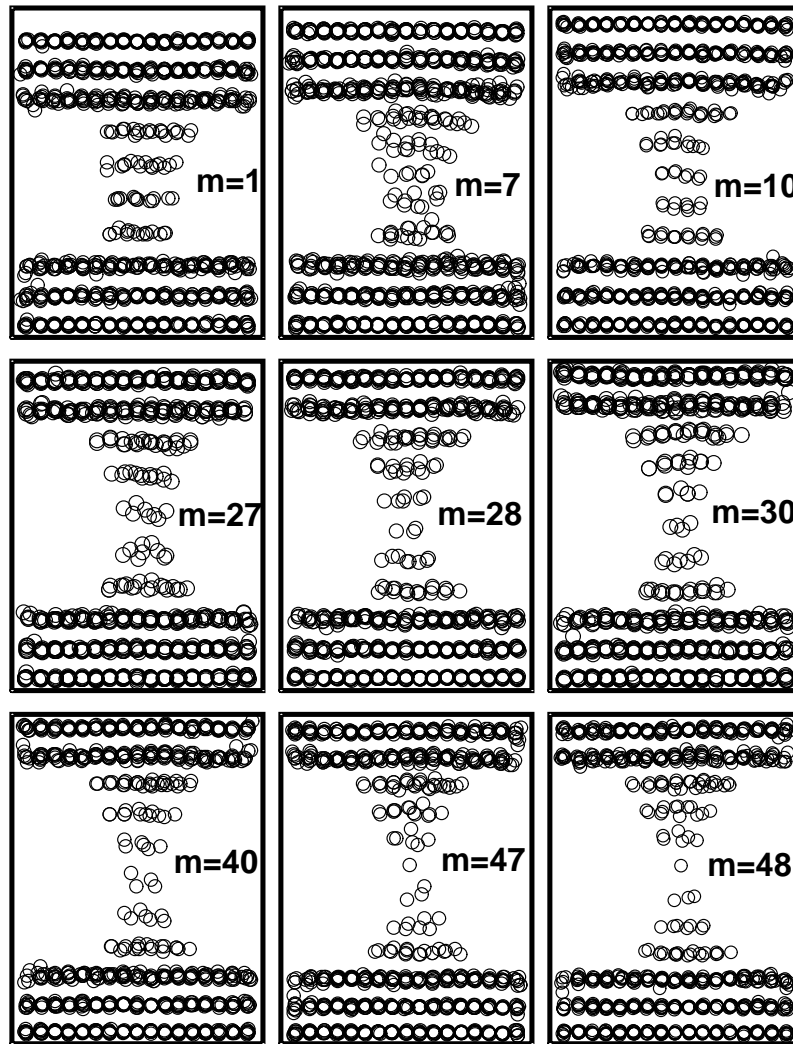


**Figure 2.** Snapshots of the side view of the atomic structure for the relevant steps of stretching  $m$ .  $J_1$ ,  $J_2$  and  $J_3$  occur at  $m = 10$ , 28 and 48, respectively.

that persists until  $m = 57$  before the breaking occurs.

The mechanical and electrical properties of the neck made of a single Cu atom are quite different and strongly dependent on the bonding geometry, i.e. the position of this single atom relative to atoms in adjacent layers. An earlier study [17] based on SCF total energy calculations carried out by using an *ab initio* pseudopotential method showed that a single Al atom between two metal surfaces is stabilized through interactions with surface atoms. As the nanowire is stretched, the potential well for the binding of a single atom between two flat surfaces first becomes shallower and flatter, and then a barrier develops at the flat bottom. In this way the single-well structure evolves into a double-well structure. Initially, the height of the barrier  $Q$  is small and allows the single atom to tunnel between the two wells. Eventually, the wells and barrier become pronounced with increasing stretching, so the single atom starts to stay in just one of the wells. This is taken as the beginning of the

breaking. However, if the single atom is allowed to move transversely in the  $(xy)$ -plane, it can find a local minimum by changing its registry from the H site to the (top) T site. In this way, the single atom forms a chain by facing the atoms on both nearest layers and provides further elongation.

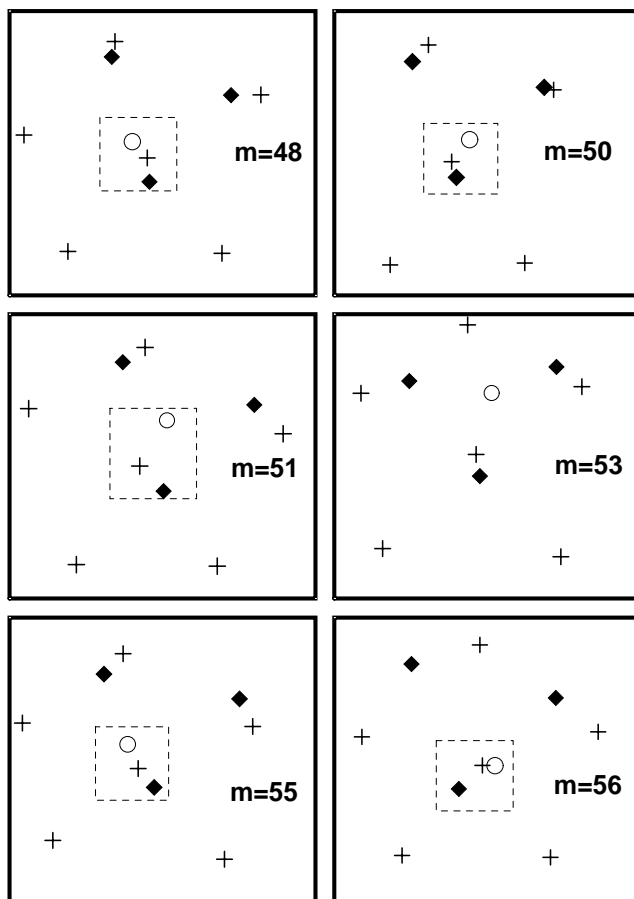


**Figure 3.** Top views of the atomic structures in three adjacent layers of the central region of the neck for the final stages of the stretching. The formation of an atomic chain is highlighted by a dashed box. The atom indicated by an open circle ( $\circ$ ) is located at the narrowest part of the neck. Atoms indicated by plus signs (+) and diamonds ( $\diamond$ ) lie in the adjacent layers below and above, respectively.

It becomes clear from the above discussion that if we exclude the yielding stage which gives rise to some kind of disorder at the neck, the layer structure is preserved over the course of the stretching. Here the layer structure denotes the atoms that lie within a space of finite thickness ( $\Delta l \sim 0.2 \text{ \AA}$ ) and are well separated from the adjacent layers. In this respect, the registry of atoms relative to adjacent layers is a crucial feature as regards specifying distorted layers. The H-site registry usually lowers the energy. However, under continuing stretching, the two-dimensional (2D) square lattice of the Cu(001) planes is gradually distorted, and it changes into a 2D hexagon-like structure with increasing interlayer separation. In this situation, the atomic structure of the layer is changing as if it is transforming to the (111) plane of the fcc lattice, so different layers face different H sites. Beyond a certain value of

stretching, the T-site registry may be favoured, and hence it appears as a local minimum in the Born–Oppenheimer surface. Such situations are shown in figure 3 for  $m = 48$ –56. Note the formation of a chain between *three*-atom and *six*-atom layers for  $m = 48$ . While the *six* atoms form a centred pentagon, the chain goes through the centre (see the panel for  $m = 48$  in figure 3). The transition from the H-site registry to the T-site registry and hence the formation of a chain structure have important implications: the binding structure of atoms and hence the electronic states change upon the formation of the chain structure. In particular, the energy of the  $n$ th state  $\epsilon_n$ , that is localized at the single neck atom, relative to  $E_F$  is crucial in the formation of the current-transporting states between two parts of the nanowire. Earlier, we showed that the conductance of the neck increases with stretching shortly before the breaking owing to the increase of the local density of states  $L(E_F)$  upon formation of the atomic chain [9]. *Ab initio* calculations revealed that not only the electronic structure but also the mechanical properties of the atomic chain are significantly different from those of the bulk [16].

The yielding and fracture are expected to depend on the initial diameter, the shape of the wire, the stretching rate and the temperature. Here we investigate these effects on the tn and ttn wires, whose initial cross-sections are already small and incorporate only 4–5 atoms in the same Cu(001) planes. At 300 K individual atoms migrate from the central region of the neck towards the ends. This already provides some necking before significant stretching has occurred. Interestingly, in recent experiments a gold nanowire was broken after the stretching had already stopped; this suggests that necking can develop by itself in thin wires [18]. As a result of the surface migration of atoms the profile of the wire becomes smooth and horn-like even if the connection of the cylindrical neck to the ends is initially discontinuous. The migration of neck atoms at elevated temperatures proceeds more easily. The stretching of the tapered nanowire (the ttn wire), which has the same initial cross-section as the tn wire but a smooth and conical connection to the end layers, leads to faster necking and fewer jumps in the  $F_z(m)$  curve.

The effect of temperature and the increments  $\Delta z$  are investigated for the ttn nanowire. The stretch at 1 K exhibits much sharper jumps of  $F_z$  indicating that the structure is more rigid at low temperature during the elastic stage. In contrast to the case for pulling at room temperature, the atoms of the neck are usually disordered during the stretching at  $T = 1$  K. The layer structure is recovered only for a short time after a new layer is formed. The effect of the increment is investigated by pulling a nanowire (the ttn wire) from both ends at  $T = 300$  K with  $\Delta z = 0.05, 0.1$  and  $0.15$  Å. The results for  $\Delta z = 0.05$  and  $0.1$  are essentially the same, and exhibit well defined jumps in the force versus stretch curve. For the case where  $\Delta z = 0.15$  Å, the wire breaks before the new layer has formed, however.

#### 4. Conductance

Electrons can be transported ballistically from one metal electrode (or reservoir 1) to the other (reservoir 2) if a current-transporting state(s)  $\Psi_i$  at  $E_F$  is (are) formed in the constriction or in a point contact between these electrodes. If the cross-section of the constriction varies slowly and its potential  $V(r)$  is uniform, the current-transporting states have unique (and uniform) energy quantization along the constriction  $\epsilon_i(z)$  in the adiabatic limit. Then each current-transporting state  $\Psi_i$  of  $n$ -fold degeneracy can be viewed as an independent,  $n$ -fold conduction channel. The conductance increases by  $n(2e^2/h)$  when this channel is opened. In this way the variation of  $G$  with the contact area ( $A$ ) in the narrowest part of the neck or with  $E_F$  displays a sharp step structure with flat plateaus between consecutive steps if the tunnelling and mixing between channels are negligible. A



sharp step structure of  $G$  with sudden changes in terms of exact integer multiples of  $2e^2/h$  is usually taken as a manifestation of the quantization of conductance (in spite of the fact that it is not the conductance, but the current-transporting states that are quantized in the wire or constriction). The channels are mixed by a finite temperature and a bias voltage, and also by scattering due to potential nonuniformities (such as saddle-point potentials, discontinuous changes of the diameter and surface roughness) and impurities. These cause the sharp step structure to fade away [2, 9]. Sharvin's regime [19] is another extreme case in which the length of the constriction vanishes, i.e.  $l \rightarrow 0$ , and the step structure is almost totally smeared out and the plateaus disappear.

As far as the electron transport is concerned, the metal nanowires in figure 2 can be viewed as a constriction (or connective neck) in which  $V(r) < E_F$ . The current-transporting states would have a level spacing of  $\sim 1$  eV if  $l$  was larger than  $\lambda_F$  and the radius of the wire was in the region of  $\lambda_F$  [2, 16]. If the radius and hence  $A$  were either uniform or slowly varying with  $z$  and also the diameter changed continuously with the stretching, the  $G(s)$  curve would show a sharp step structure and flat plateaus without significant channel mixing at room temperature. It is apparent that the atomic structure of the stretching wires shown in figure 2 does not comply with the above ideal conditions and is far from adiabatic limit. Since the length of the narrowest part of the neck (which can be taken as uniform) is smaller than  $\lambda_F$ , the contribution of tunnelling is significant, so the sharp step structure is smeared out and the plateaus disappear. Furthermore,  $V(r)$  is expected to be nonuniform and greatly roughened in the wire. In these circumstances, the channels can mix significantly. Of course, the transverse quantization of states in the constriction will be reflected in the  $G(s)$  curve, especially when the radius is in the region of  $\lambda_F$  (as in metal nanowires with very small cross-sections including just a few atoms). The sharp step structures and flat plateaus are, however, expected to disappear; the opening of the channels is delayed and thus  $G$  attains values lower than integer multiples of the quantum conductance [2, 20, 21]. The conditions shortly before the breaking occurs, in which the neck consists of a single atom (or a short atomic chain), present a rather interesting situation. Owing to the reduced interaction at large interatomic separation (corresponding to  $m \geq 48$  in figure 2), the transversely quantized constriction state(s) is (are) derived from the states of the single atom in the neck. If the energy of the  $n$ -fold constriction state  $\epsilon_i$  is slightly offset from  $E_F$ , the conductance is smaller than  $n(2e^2/h)$ , but is still significant due to the resonance broadening of  $\epsilon_i$  in the metallic density of states [9]. When this state is aligned with states of the electrode at  $E_F$ ,  $G(s)$  increases to  $n(2e^2/h)$ . This is similar to the resonant tunnelling condition proposed earlier [17, 21].

It becomes clear that the  $G(s)$  curves obtained from the experiments [3–6] are rather different from those obtained in the adiabatic limit. In view of the earlier theoretical arguments [10, 11] and recent force and conductance measurements [7, 8], the understanding of the ballistic electron transport through metal nanowires, in particular the interpretation of the features of  $G(s)$ , requires a calculation of the conductance using the detailed atomic structure. To this end, we use the structures calculated by the present MD simulations and generate the potential  $V(r)$  in the wire by the linear combination of atomic potentials.

First we calculated the potential of a free Cu atom,  $V_p(r)$ , from the generalized norm-conserving pseudopotential given by Hamann's programme [22]. We next generated a screened potential  $V_a(r)$  from  $V_p(r)$  by taking the screening of the metallic Cu into account. This potential,  $V_a(r)$ , is illustrated in inset (a) of figure 4. The potential of the wire at a given  $s$  is constructed from linear combination of the  $V_a(r)$ :

$$V_s(\mathbf{r}) = \sum_i V_a(|\mathbf{r} - \mathbf{R}_i(s)|) \quad (2)$$

where the  $\mathbf{R}_i(s)$  are the atomic positions obtained from the MD simulations for a given value of  $s$ ; the index  $i$  runs over all of the atoms in the neck. In order to use the cylindrical symmetry,  $V_s(\mathbf{r})$  is symmetrized around the axis passing through the centre of gravity of the neck along the  $z$ -direction. This potential is transformed into a finite-wall cylindrical potential by performing a radial averaging and then a least-squares fit.

Moreover, in order to make computations of transverse states feasible, the walls of  $V_s(\mathbf{r})$  are taken as infinite. In this modification of  $V_s(\mathbf{r})$ , the relaxation of the transverse wave and hence also the downward shift of the corresponding energy eigenstates in the finite-wall potential are taken into account by increasing the radius  $\rho = (x^2 + y^2)^{1/2}$  at any  $z$  so that the eigenenergies of the ground states of the two potentials match. Eventually, the potential of the wire reads

$$V_s(\rho, z) = \begin{cases} \phi_s(z) & \rho \leq \rho_s(z) \\ \infty & \rho \geq \rho_s(z). \end{cases} \quad (3)$$

The above potential includes various effects. In particular, the saddle-point potential  $\phi_s(z)$  is an essential ingredient that was omitted in earlier calculations carried out in the study of conductance in metal nanowires. The neck profile is shown in inset (b) of figure 4 for the stretching step  $m = 38$ . We calculate the conductance of the Cu nanowire (that is specified by the number of stretching steps,  $m$ , that it undergoes) by using the transfer matrix method. To this end, we divide the potential into discrete segments of equal widths, and assume that in each segment  $z_l < z < z_{l+1}$ ,  $\phi_s(z)$  and  $\rho_s(z)$  have uniform values obtained by averaging therein. Then the longitudinal wave functions  $\exp(i\gamma_{n_l}^s(z))$  and circularly symmetric transverse eigenstates  $\varphi_{n_l}^s(\rho; z)$  are obtained for each segment with

$$\gamma_{n_l}^s(z) = \left\{ \frac{2m}{\hbar^2} [E - \phi_s(z) - \epsilon_{n_l}^s(\rho; z)] \right\}^{1/2} \quad (4)$$

where  $\epsilon_{n_l}^s(\rho; z)$  is the eigenenergy of  $\varphi_{n_l}^s(\rho; z)$ . Starting with an incident plane wave  $e^{ik_j \cdot r}$  for  $z \leq 0$ , we express the current-transporting states in each segment  $z_l < z < z_{l+1}$  in terms of linear combinations of the longitudinal and transverse states, and determine the coefficients by means of multiple boundary matching. The current and hence also the conductance are calculated by means of an appropriate summation of the current over the states at the Fermi surface.

The calculated variation of  $G(s)$  corresponding to the structures leading to the  $F_z(s)$  curve in figure 1 is illustrated in figure 4. The overall behaviour of  $G(s)$  is reminiscent of the experimental data [3–6] and reflects the correlation with  $F_z(s)$  revealed by the experimental studies [7, 8]. The sudden changes of  $G(s)$  (which were erroneously attributed to the quantum steps in some earlier publications) are associated in fact with the abrupt reductions of the neck marked by  $J_1$ ,  $J_2$  and  $J_3$  in figure 1. A similar conclusion has been derived from the recent conductance calculation that employs an orthonormal nearest-neighbour 1s tight-binding model with a half-filled band [23], and uses the atomic configurations obtained by the MD simulation of Au wire performed at  $T = 1$  K. The plateau-like structure occurs only in the last two steps in figure 4. The conductance calculated before the breaking occurs, for  $46 < m < 57$ , is approximately 40% of  $2e^2/h$  and hence is smaller than the experimental value. This is due to the fact that we used the bulk screening length in calculating the potential of all types of neck obtained in the course of the stretching. This, of course, is not appropriate for a single-atom neck, and causes  $\phi_s(z)$  to rise as a result of over-screening. In fact, the lowering of  $\phi_s(z)$  by  $\sim 2$  eV causes the first channel to open and leads to  $G \sim 2e^2/h$ . This situation provides more evidence that the properties of a metal nanowire deviate from those of the bulk when its diameter is reduced to  $\sim 2$ – $3$  Å.

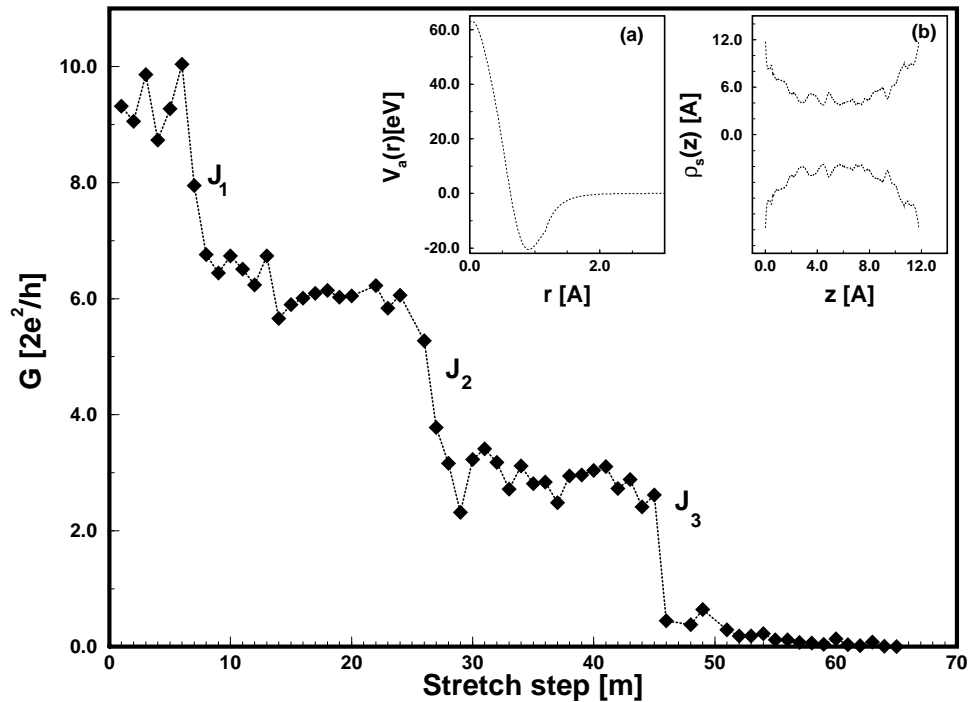


**Figure 4.** The conductance versus the number of stretching steps calculated by using the potential described by equation (3) in the text.  $J_1$ ,  $J_2$  and  $J_3$  are the abrupt structural changes indicated in figure 1. The atomic pseudopotential and the profile of the neck corresponding to  $m = 38$  are shown in insets (a) and (b), respectively.

Some features of  $G(s)$  are closely correlated with the detailed atomic structure of the neck at a given value of  $s$ . For example, the dip of  $G(s)$  at  $m = 28$  is related to the neck which included a new layer at the end of the yielding during  $J_2$ . Initially, this new layer comprised only three atoms, so  $G(s)$  was only slightly larger than  $2(2e^2/h)$ . However, after a short while ( $m > 30$ ), the cross-section of this layer was increased by the migration of a single atom from an adjacent layer, and hence the conductance rose to  $\sim 3(2e^2/h)$ . Clearly, the measured conductance is strongly dependent on the detailed atomic structure, in particular the number and configuration of atoms in the narrowest layer. Accordingly, significant conductance fluctuations are expected to occur in the quasi-elastic stage (before any yielding), even when the stretching is completely frozen. At this point, we note that  $G(s)$  is not uniform and does not form a flat plateau for  $30 \leq m \leq 45$  where the neck is made from four atoms; the configuration of these atoms is crucial as regards the calculated conductance. In the early stage, for  $10 < m < 17$ , the  $G(s)$  curve slopes considerably and does not form a plateau. Another point that we emphasize is the profile of the neck displayed in inset (b) of figure 4. In spite of a certain averaging effect, it is still greatly roughened.

## 5. Conclusions

The atomic rearrangements that occur during the pull-off of a metal nanowire have been shown to be crucial as regards electrical and mechanical properties. In agreement with earlier

theoretical and experimental studies, the variation of the force with the stretching displays two consecutive stages, i.e. quasi-elastic and yielding stages. The layer structure persisted during the quasi-elastic stage; the relocation of atoms within a layer and also single-atom exchange between layers cause fluctuations and deviations of  $F_z(m)$  from a linear variation. The layer structure that is destroyed at the beginning of the yielding stage is recovered by a new layer with a smaller cross-section forming. This leads to a sudden reduction of the neck and a sudden reduction of the force. However, the cross-section of the neck can even increase temporarily, owing to the migration of an atom from an adjacent layer. The 2D square-lattice structure of the ideal Cu(001) planes becomes distorted with increasing tensile strain. As the interlayer interaction weakens, it shows a tendency to change into a 2D hexagonal structure (i.e. a close-packed structure like that of the (111) plane in the fcc lattice). For a moderate level of stretching, the H-site registry is maintained; it changes to T-site registry at the high level of stretching encountered shortly before the breaking occurs. Eventually, short atomic chain(s) are formed at the neck. At low temperature (1 K),  $F_z$  exhibits much sharper jumps, and the atoms of the neck are usually disordered during the stretching. It is also predicted that the neck can develop by itself in the Cu nanowires having small cross-sections and consisting of 3–5 atoms.

The conductance curve,  $G(s)$ , calculated by using a realistic potential constructed for the atomic structures obtained from MD simulations, is well correlated with the tensile force curve,  $F_z(s)$ . In agreement with our earlier arguments, the present results demonstrate that abrupt changes of the cross-section of the neck lead to abrupt changes in the  $G(s)$  curve. Even if the number of atoms in a neck layer is fixed,  $G$  depends on the atomic configuration. Furthermore, our calculations lead to the conclusion that the behaviour of a single-atom neck is quite different from that of a wide neck. We finally point out that the behaviour of  $G(s)$  for a nanowire reflects the transverse quantization of electronic states in the neck rather than the quantization of the conductance.

## References

- [1] Gimzewski J K and Möller R M 1987 *Phys. Rev. B* **36** 1284  
Gimzewski J K, Möller R M, Pohl D W and Schlittler R R 1987 *Surf. Sci.* **189** 15  
Dürig U, Gimzewski J K and Pohl D W 1986 *Phys. Rev. Lett.* **57** 2403
- [2] Tekman E and Ciraci S 1991 *Phys. Rev. B* **43** 7145 and references therein
- [3] Agrait N, Rodrigo J G and Vieira S 1993 *Phys. Rev. B* **47** 12 345
- [4] Landman U, Luedtke W D, Burnham N A and Colton R J 1990 *Science* **248** 454  
Pascual J I, Méndez J, Gómez-Herrero J, Baró A M, Garcia N, Landman U, Luedtke W D, Bogachek E N and Cheng H P 1995 *Science* **267** 1793
- [5] Olesen L, Lægsgaard E, Stensgaard I, Besenbacher F, Schiøtz J, Stoltze P, Jacobsen K W and Nørskov J K 1994 *Phys. Rev. Lett.* **72** 2251  
Olesen L, Lægsgaard E, Stensgaard I, Besenbacher F, Schiøtz J, Stoltze P, Jacobsen K W and Nørskov J K 1995 *Phys. Rev. Lett.* **74** 2147
- [6] Krans J M, Muller C J, Yanson I K, Govarent Th C M, Hesper R and Ruitenbeek J M 1994 *Phys. Rev. B* **48** 14 721  
Krans J M, Muller C J, Van der Post N, Postama F R, Sutton A P, Todorov T N and Ruitenbeek J M 1995 *Phys. Rev. Lett.* **74** 2146
- [7] Agrait N, Rubio G and Vieira S 1995 *Phys. Rev. Lett.* **74** 3995  
Rubio G, Agrait N and Vieira S 1996 *Phys. Rev. Lett.* **76** 2302
- [8] Stalder A and Dürig U 1996 *Appl. Phys. Lett.* **68** 637
- [9] Mehrez H, Ciraci S, Buldum A and Batra I P 1997 *Phys. Rev. B* **55** R1981
- [10] Ciraci S and Tekman E 1989 *Phys. Rev. B* **40** 11 969  
Ciraci S 1990 *Tip-Surface Interactions in Scanning Tunnelling Microscopy and Related Methods* vol 184 (Kluwer: Academic) p 113
- [11] Todorov T N and Sutton A P 1993 *Phys. Rev. Lett.* **70** 2138

- [12] Bratkovsky A M, Sutton A P and Todorov T N 1995 *Phys. Rev. B* **52** 5036
- [13] Sutton A P 1996 *Curr. Opin. Solid State Mater. Sci.* **1** 827
- [14] Erkoç Ş 1994 *Z. Phys. D* **32** 257  
Özdoğan C and Erkoç Ş 1997 *Z. Phys. D* **41** 205  
Morse M D 1986 *Chem. Rev.* **86** 1049
- [15] Sutton A P and Pethica J B 1990 *J. Phys.: Condens. Matter* **2** 5317
- [16] Mehrez H 1996 *MSc Thesis* Bilkent University  
Mehrez H and Ciraci S 1997 *Phys. Rev. B* **56** at press
- [17] Ciraci S, Tekman E, Baratoff A and Batra I P 1992 *Phys. Rev B* **46** 10411
- [18] Muller C J, Krans J M, Todorov T N and Reed M A 1996 *Phys. Rev. B* **53** 1022
- [19] Sharvin Yu V 1965 *Zh. Eksp. Teor. Fiz.* **48** 984 (Engl. Transl. 1965 *Sov. Phys.-JETP* **21** 655)
- [20] Kander I, Imry Y and Sivan U 1990 *Phys. Rev. B* **41** 12941
- [21] Tekman E and Ciraci S 1989 *Phys. Rev. B* **40** 8559
- [22] Hamann D R 1989 *Phys. Rev. B* **40** 2980
- [23] Todorov T N and Sutton A P 1996 *Phys. Rev. B* **54** R14234